International Journal of Chemical and Biochemical Sciences
(ISSN 2226-9614)
Journal Home page: www.iscientific.org/Journal.html

Hydrochemical assessment and spatiotemporal variation of groundwater quality in coastal aquifer: Sudr area, South Sinai, Egypt

Mohamed Shehata[1], Ehab Zaghlool[2], Ahmed Sedik[3*] and Ahmed M. Nosair[3]

1- Geology Department, Faculty of Science, Zagazig University, Zagazig, 44519, Egypt
2- Hydrogeochemistry Department, Desert Research Center, Al-Matariya, Cairo 11753, Egypt
3- Environmental Geophysics Lab (ZEGL), Geology Department, Faculty of Science, Zagazig University, Zagazig 44519, Egypt

Abstract

The quality of groundwater in coastal aquifers is at risk in numerous regions worldwide due to seawater intrusion (SWI). The objective of this research is to analyze the condition of the Quaternary aquifer in the Sudr region of South Sinai, Egypt, and evaluate the suitability of groundwater quality for irrigation from 1996 to 2022 by utilizing hydrochemical indicators. The Western and North-Western regions exhibit high salinity levels, with a gradual decrease towards the east. The predominant water types identified in the study region include Na-Cl, Ca Mg-Cl, and Ca-Cl type. The Hydrochemical Facies Evolution Diagram (HFE-D) revealed that the area impacted by the seawater intrusion to 73.33%. The findings of spatiotemporal variation based on sodium adsorption ratio (SAR), sodium percentage (Na%), and permeability index (PI) suggest that groundwater quality for irrigation deteriorated in 2022 compared to 1996. According to the SAR data, the percentage of samples classified as excellent decreased from 71.95% in 1996 to 58.33% in 2022, with an increase in the classification of samples as good. This research contributes to the ongoing monitoring of groundwater quality in coastal aquifers, providing valuable information for decision-makers.

Keywords: Hydrogeochemistry, Seawater intrusion, Irrigation, Coastal aquifer, HFE-D, spatiotemporal variation

Full length article **Corresponding Author*, e-mail: ahmedsedik@zu.edu.eg

1. Introduction

Groundwater serves as a key irrigation source in coastal aquifers. The over-extraction of groundwater from these aquifers often exceeds the rate of natural replenishment, causing a hydrochemical imbalance. As a result, seawater begins to intrude laterally into the coastal area and saltwater moves upwards inland [1,5]. Salinization in aquifers due to seawater intrusion, worsened by excessive extraction of groundwater [6,10]. An estimated 40% of the world's population currently lives within 100 kilometers of the coasts, a number projected to rise due to escalating tourism, internal migration, and rapid population expansion [11,12]. The Quaternary aquifer, composed of alluvial sediments, is anticipated to support agricultural growth in the Suez Gulf area [13]. This aquifer is recognized for its substantial groundwater potential, rendering it the most efficient aquifer in the Gulf of Suez Rift [14].

SWI often results in the natural contamination of freshwater areas close to the shore, consequently affecting the quality of water [15,16]. Furthermore, excessive extraction of groundwater in the South Sinai Peninsula, specifically in the Ras Sudr coastal aquifer, has resulted in considerable salinization of the groundwater [17,20]. The hydrochemical analysis offers valuable insights regarding the groundwater's appropriateness [21].

It is crucial to guarantee a high standard of water quality for irrigation to preserve current agricultural production and safeguard sensitive crops [22]. Regular monitoring of groundwater quality is crucial and should be consistently implemented [23]. Many researchers have conducted studies to assess groundwater quality by utilizing various irrigation indices [24,27].

The main goal of this study is to i) utilize GIS to analyze the spatial distribution variations of major ions and salinity ii) identify the hydrochemical facies in the area iii) determine the spatiotemporal variation during the periods 1996 and 2022 for evaluating groundwater quality and its appropriateness for irrigation purposes. This research aims to assist decision-makers and planners in the monitoring of the aquifer's groundwater quality.

2. Study area

The study area is Sudr area that is situated in the southwest region of the Sinai Peninsula on the eastern side of the Gulf of Suez, between latitudes 29°42'57.99" to 29°36'11.99"N and longitudes 32°41'53.99" to 32°43'21.39"E (Fig. 1). Wadi Sudr and Wadi Lahata are in the delta of region. This area is conveniently accessible from the city of Suez to the north via the El Tor coastal highway, to the south through the Sudr El Hitan Mountain paved road. The absence of fresh water in the Wadi Lahatah delta is due to its proximity to seawater. This is caused by the existence of Sabkha and playa deposits (salt evaporites) below the wadi deposits (alluvium aquifer) [28]. Furthermore, the Wadi Sudr delta hosts brackish, saline to highly saline water, with a noticeable absence of freshwater. This occurrence is attributed to leaching and dissolution processes originating from coastal salt deposits and agricultural practices, causing saltwater intrusion in the groundwater. The main source of water for irrigation and household purposes comes from the shallow alluvium aquifer [28].

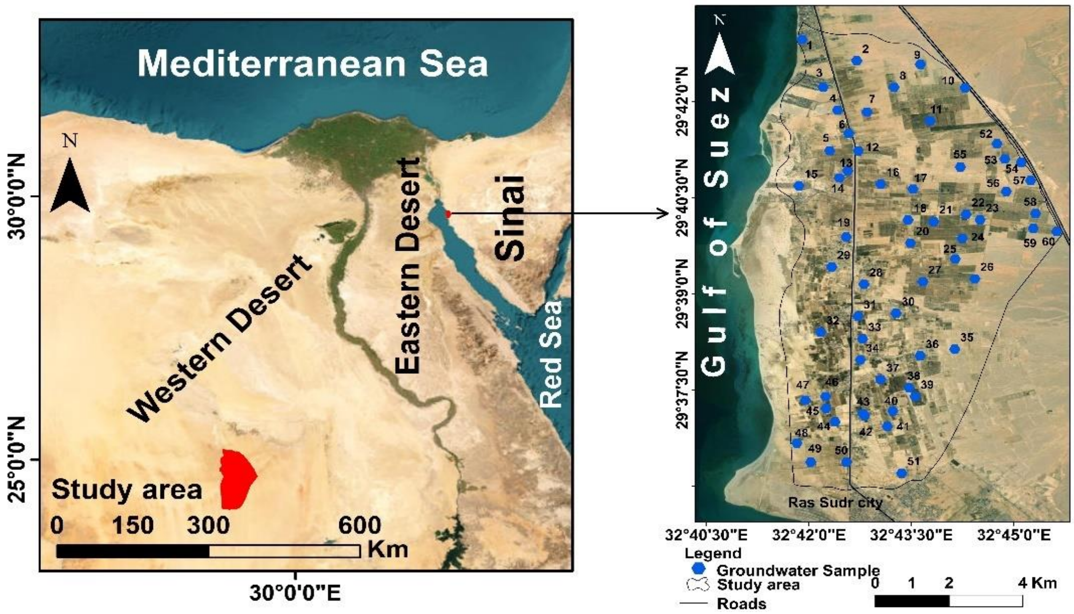

Figure 1: Sampling location of the study area.

The drilled wells in the study area are characterized by the presence of Quaternary alluvium deposits in their subsurface lithology [29] (Fig. 2).

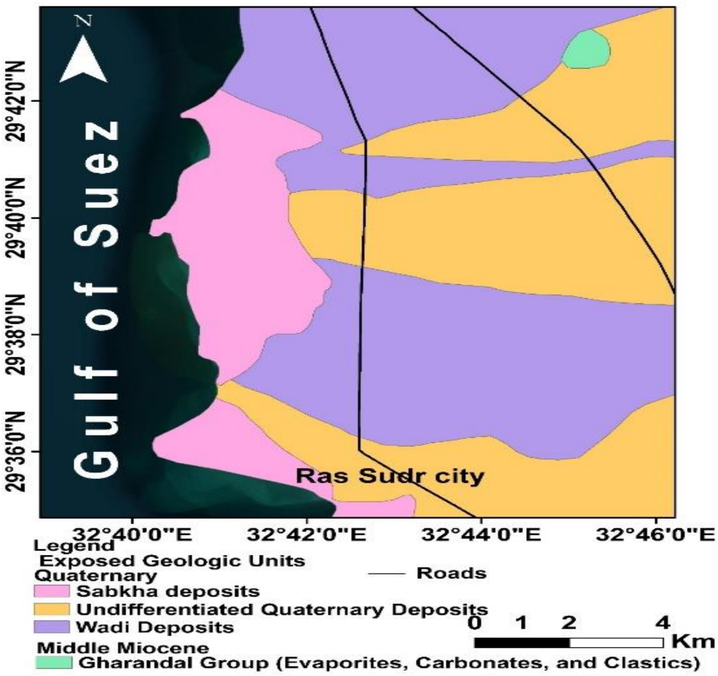

Figure 2: Geological setting of the study area [30].

The Pleistocene and Holocene sediments are in the main channels of the catchment and the Wadi Sudr delta, primarily consisting of alluvial deposits with different sizes of dolomitic limestone boulders spread throughout the Wadi's main pathway. The distance from the water divide is directly correlated with the size of the Wadi fills deposits [31]. The primary aquifer in the investigated region is the Quaternary aquifer [32,33]. The thickness of Quaternary deposits exhibits notable variability along the course of the wadis flowing through Gebel Sin Bishr and Gebel El Raha, with depths measuring less than 5 meters at the outlets [31]. The aquifer comprises two layers, with the upper layer consisting of 14 meters of gravel and medium sand, and the lower layer containing over 17 meters of sporadic gravel, sand, clay, and sandstone, separated by intermittent shales with a lenticular shape exhibiting varying thickness and well-defined extension. As a result, the aquifer is classified as an unconfined single layer [34]. The hydraulic gradient varies between 0.0009 and 0.01, while the storativity varies from $3.6*10^{-2}$ to $4.2*10^{-2}$ [13]. Additionally, the average hydraulic conductivity is 96.28 m/day, transmissivity ranges from 1054 to 10328 m^2/day, and specific capacity varies between 3.5 and 78 m^3/h/m [35]. In the autumn and winter seasons, the notable annual direct rainfall of 13.36 mm [36] leads to substantial flash floods [18,28]. The eastward subsurface flow of the Miocene aquifer, amounting to 2.7*106 m^3/year, plays a significant role in recharging the groundwater [36].

3. Materials and Methods

3.1. Analytical procedure

During a February 2022 field trip in the Sudr area, 60 groundwater samples were collected from production wells accessing the Quaternary aquifer at depths varying between approximately 10 m to 65 m. Each sample corresponds to a specific well, as illustrated in Figure 1. The samples were collected in polyethylene bottles that had been cleaned with 5% nitric acid (HNO_3) and rinsed with distilled water from the wells after pumping for 25 minutes to ensure the samples accurately reflected the groundwater chemistry. The samples were gathered in the field and their locations were pinpointed using a GPS system, then plotted on a map (Fig. 1). The samples were stored in an ice box maintained below 5 °C before being transported to the laboratory for analysis. Field measurements, such as electrical conductivity (EC), TDS, pH, and temperature, were conducted using a portable field kit due to the variability of these parameters over time during storage.

Major ion chemical analyses, including calcium, magnesium, sodium, potassium, bicarbonate, sulfate, and chloride, were conducted at the Environmental Geophysical Lab (ZEGL) at Zagazig University in Zagazig, Egypt. Concentrations of Na+ and K+ were measured utilizing a Flame Photometer (Model: PFP7) [37–39]. Standard and blank solutions are prepared and analyzed after every ten samples in a repeated manner. Chemical analyses were conducted following the standard procedures of [40–42]. The analytical precision was attained by calculating the ionic balance error (IBE) for ions measured in meq/l, ensuring that the error rate was within ±5% [43]:

$$IBE = \frac{\sum \text{Cations} - \sum \text{Anions}}{\sum \text{Cations} + \sum \text{Anions}} * 100$$

According to IBE standards, the water quality assessment is deemed valid within a tolerance range of 5% [40]. All chemical variables are reported in milligrams per liter (mg/L), except for pH and EC. The EC value is denoted in micro-mhos per centimeter (µS/cm) at a temperature of 25°C.

3.2. Total hardness (TH)

Total hardness is indicated by the combined concentrations of Ca^{2+} and Mg^{2+}, which are measured in parts per million (ppm) of $CaCO_3$. According to Todd and Mays (2004), the presence of divalent metallic cations is the main contributor to groundwater hardness. Todd and Mays [44] determined the total hardness (TH) in mg/l as:

$$TH = 2.497 * Ca^{2+} + 4.115 * Mg^{2+}$$

3.3. Sodium adsorption ratio (SAR)

The ratio of sodium to calcium and magnesium ions in water, known as the SAR, is commonly used as a key indicator to assess the quality of groundwater for irrigation purposes [45]. The SAR is often used as an indicator of the threat posed by sodium/alkali, as indicated by [46] as shown in the equation:

$$SAR = \frac{Na^{+}}{\sqrt{\frac{Ca^{2+} + Mg^{2+}}{2}}}$$

The levels of sodium (Na^+), calcium (Ca^{2+}), and magnesium (Mg^{2+}) ions in irrigation water are denoted in milliequivalents per liter (meq/l), while SAR is indicated as (millimoles per liter)$^{0.5}$.

3.4. Sodium Percentage (Na %)

The sodium content percentage in natural waters is a critical factor in determining its suitability for agricultural purposes. When sodium combines with carbonate, it can cause the formation of alkaline soils, while its combination with chloride can result in saline soils being created [47]. Excessive sodium in water can have adverse effects, including changing soil qualities and reducing the permeability of soil [48]. The calculation of the sodium percentage (Na %) involves the use of the formula provided below. Na % is calculated by utilizing the following formula.

$$Na^{+}\% = \frac{Na^{+} + K^{+}}{Ca^{2+} + Mg^{2+} + Na^{+} + K^{+}} * 100$$

The excessive sodium content in irrigation water causes clay particles to absorb sodium ions, displacing magnesium and calcium ions. This process diminishes soil permeability, leading to ineffective internal drainage [21].

3.5. Permeability Index (PI)

The Permeability Index (PI) reflects the level of impact on soil permeability. With regular use of irrigation water containing ions like Na^+, Ca^{2+}, Mg^{2+}, and HCO_3^-, the soil's permeability gradually reduces over time [49]. Doneen [50] established the permeability index (PI) to evaluate groundwater suitability for irrigation, with the index's definition as stated below:

$$PI = \frac{Na^{+} + \sqrt{HCO_{3^-}}}{Ca^{2+} + Mg^{2+} + Na^{+}} * 100$$

The concentrations are denoted in milliequivalents per liter.

3.6. Geographic information system (GIS) analysis

ArcGIS 10.8 was employed to produce spatial distribution images, demonstrating its effectiveness in managing and studying digital cartographic data [51]. The Inverse Distance Weighted (IDW) algorithm is used to estimate measurement values or spatially interpolate data. IDW method within the GIS spatial analyst tool is recognized for its efficacy in producing precise results [52].

4. Result and discussion

4.1. Hydrochemistry

Evaluating the quality of groundwater is essential as it is a significant factor in determining its suitability for drinking, agricultural, and industrial purposes [53]. The descriptive statistics for the collected samples are given in Table 1.

Table 1: Variation of physicochemical parameters in Sudr area.

Parameters	Min	Max	Mean
HCO_3^- (mg/l)	97.6	241	149.97
SO_4^{2-} (mg/l)	288.5	2639	1271.2
TDS (mg/l)	1321	15050	6617.43
Cl^- (mg/l)	416	7098.9	2884.63
Ca^{2+} (mg/l)	105.2	915	442.73
Mg^{2+} (mg/l)	23	572	249.22
Na^+ (mg/l)	304	3860	1641.8
K^+ (mg/l)	10	80	25.48
pH	6.8	8.2	7.46
EC (µS/cm)	3213	23500	10600

4.1.1. pH

The acidity or alkalinity of a solution is indicated by its pH, which is defined as the -log (base 10) of the concentration of hydrogen ions in moles per liter. The pH scale ranges from 0 to 14, where 7 signifies neutrality, levels below 7 denote acidity, and values above 7 indicate alkalinity. The pH values in the study area range from 6.8 to 8.2, with a mean 7.46, which aligns with the World Health Organization (WHO) standard range of 6.5 to 8.5 [54]. Higher pH values were observed in the East and specific wells (No. 2, 27, 35, 52, and 55), likely due to soil sediment leaching processes. Conversely, the lowest pH value was found in the West, attributed to seawater intrusion (Fig. 3a).

4.1.2. Total dissolved solids

Total dissolved solids (TDS) represent a method for measuring water quality. It is a measurement of the collective content of heavy metals, minerals, salts, and various organic and inorganic substances found in water. TDS levels play a vital role in identifying the quality of water and its appropriateness for different uses. Identifying groundwater is essential by analyzing its hydrochemical characteristics, particularly TDS values, to assess its suitability for a specific purpose (Table 2) [55,56]. In the Quaternary aquifer, total dissolved solids range from 1321 ppm to 15050 ppm, with an average of 6617.43 ppm.

The current research categorized the levels of groundwater salinity into four groups according to [57] that slightly saline <2000 ppm, medium saline 2000-4000 ppm, highly saline 4000-9000 ppm, and very saline >9000 ppm. The water chemistry of the studied aquifer is significantly impacted by multiple factors, such as proximity to the coastline and main wadi channel, the drilled depth below sea level, and the discharge rate. The lower TDS values in the

East are primarily due to recharge sources from surface runoff water infiltrating through flash floods, typically seen during the autumn and winter seasons (Fig. 3b). According to the predominant recharge sources, groundwater flows in the direction from east to west towards the Suez Gulf. The high TDS values in the West and North-West regions are primarily attributed to the impact of seawater intrusion, leaching and dissolution processes of Sabkha and playa, as well as Miocene deposits such as shale, anhydrite, and salt evaporites beneath the wadi deposits (alluvium aquifer). These elevated TDS levels are further exacerbated by extensive drilling of wells, consecutive evaporation from the shallow water table, and excessive withdrawal compared to the current recharge rate (Fig. 3b). Another factor that influences groundwater salinity is the evaporation from water surfaces and the dissolution of rocks [31]. The excessive pumping rates also impact the coastal area that the operational hours extend to 12 hours per day.

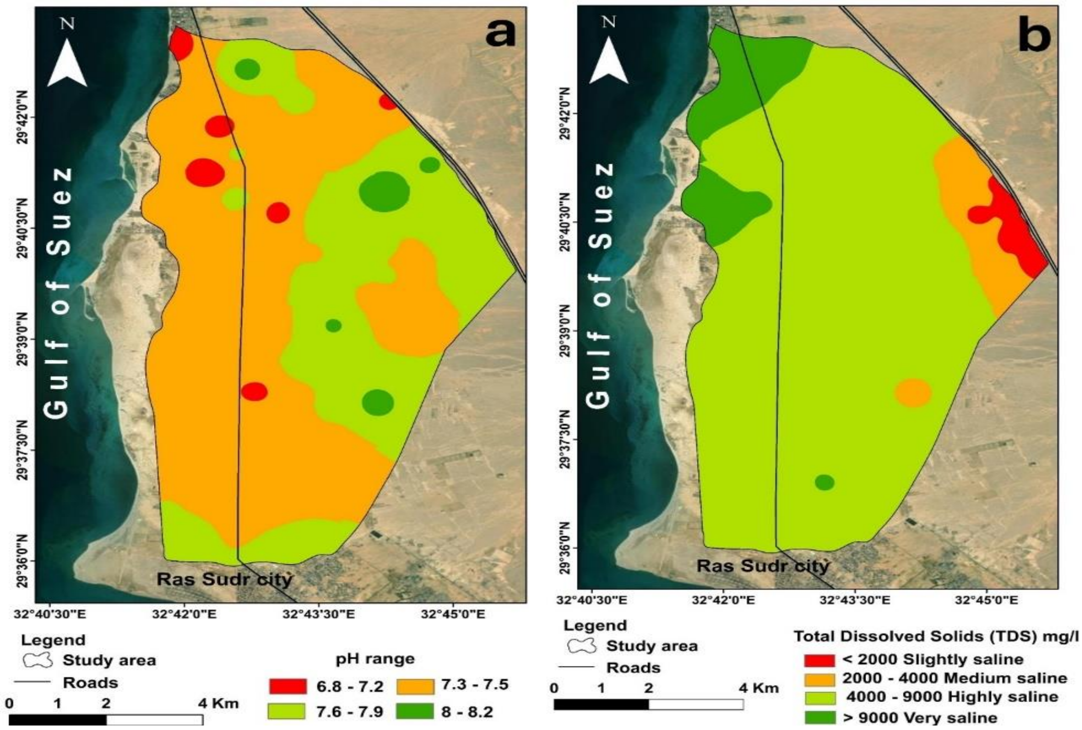

Figure 3: The spatial distribution of: **a**) pH; **b**) TDS.

4.1.3. Electrical conductivity

Electrical conductivity (EC) indicates a material's capacity for current transmission or the quantity of electrical current it can support. It varies depending on their ability to conduct electricity. The electrical conductivity in the Quaternary aquifer varies, ranging from 3213 µS/cm to 23500 µS/cm, with an average of 10599.95 µS/cm. In Figure 4a, the spatial distribution of EC is illustrated, with higher values located in the West and North-West regions and decreasing towards the east near the main Wadi channel. The significant increase in EC levels may be attributed to saltwater intrusion and the influence of sabkha deposits. EC in the study area is categorized based on the classification by [58].

4.1.4. Total hardness

The total hardness (TH) values in the area range from 423.17 ppm to 4638.54, with an average value of 2131.02 ppm. Figure 4b shows the spatial distribution of TH in the Quaternary aquifer.

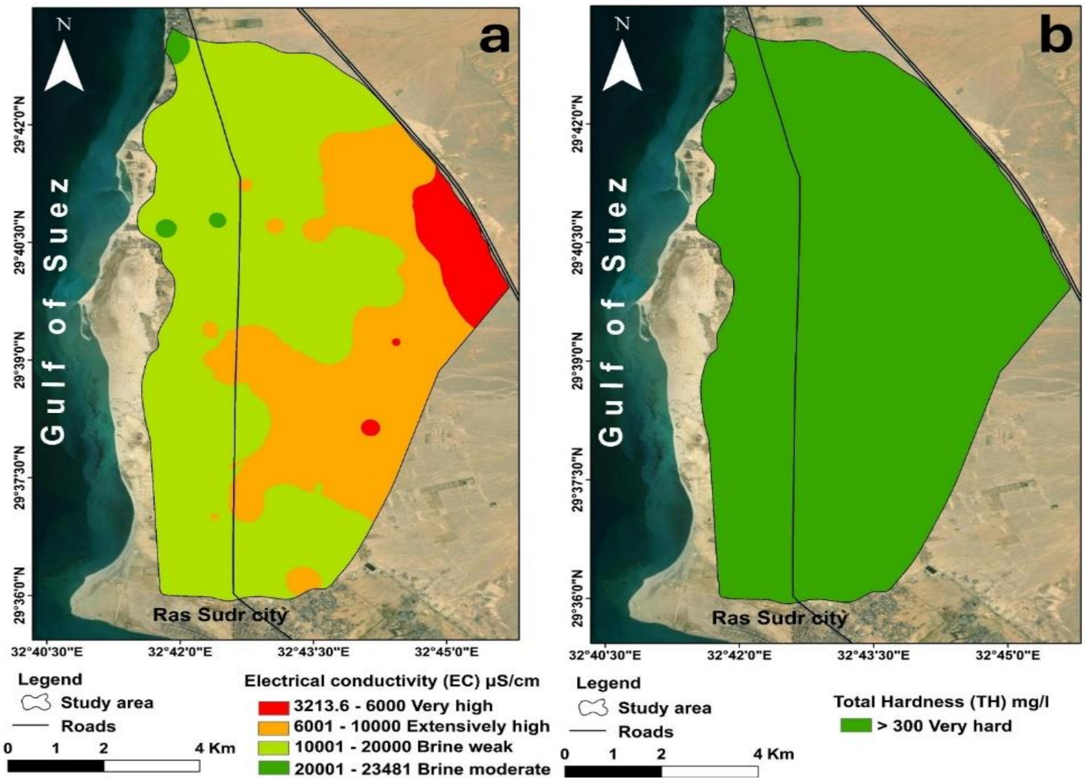

Figure 4: The spatial distribution of: **a**) EC; **b**) TH.

TH classified according to [59] that all water samples examined were determined to fall under the category of very hard water types. Figure 4b illustrates the impact of seawater intrusion, particularly in the western regions of the area, and the leaching and dissolution of salts abundant in Ca^{2+} and Mg^{2+} ions in the water-bearing formations. Additionally, it is noted that that wells tapping into the aquifer in the western and northwest regions demonstrate higher levels of hardness, whereas values decrease in the eastern parts near the primary Wadi channel due to dilution from surface and subsurface runoff. This suggests that as water salinity increases, total hardness also increases.

4.1.5. Chloride

The study area exhibits a mean chloride concentration of 2884.63 ppm, with the highest value recorded at 7098.9 ppm and the lowest value at 416 ppm. Figure 5a reflects that the total dissolved solids and chloride content exhibit a consistent trend. The chloride concentrations increase in the western and northwestern areas due to significant seawater intrusion, while they decrease in the eastern regions as the aquifer is replenished by runoff from the primary wadi channel. Chloride content can be categorized into four classes [60].

4.1.6. Sulphate

Sulfate concentrations range from 288.5 ppm to 2639 ppm, with a mean of 1271.2 ppm. Elevated levels of sulfate ions in the northwestern and western regions of the study area, indicating the presence of significant evaporite formations (such as gypsum, halite, and anhydrites) and the infiltration of seawater (Fig. 5b). In some wells within the study area, sulfate ion concentrations have increased, likely due to over-pumping and seawater intrusion. Conversely, the lowest sulfate levels were found in the eastern part of the study area, particularly near the main wadi channel.

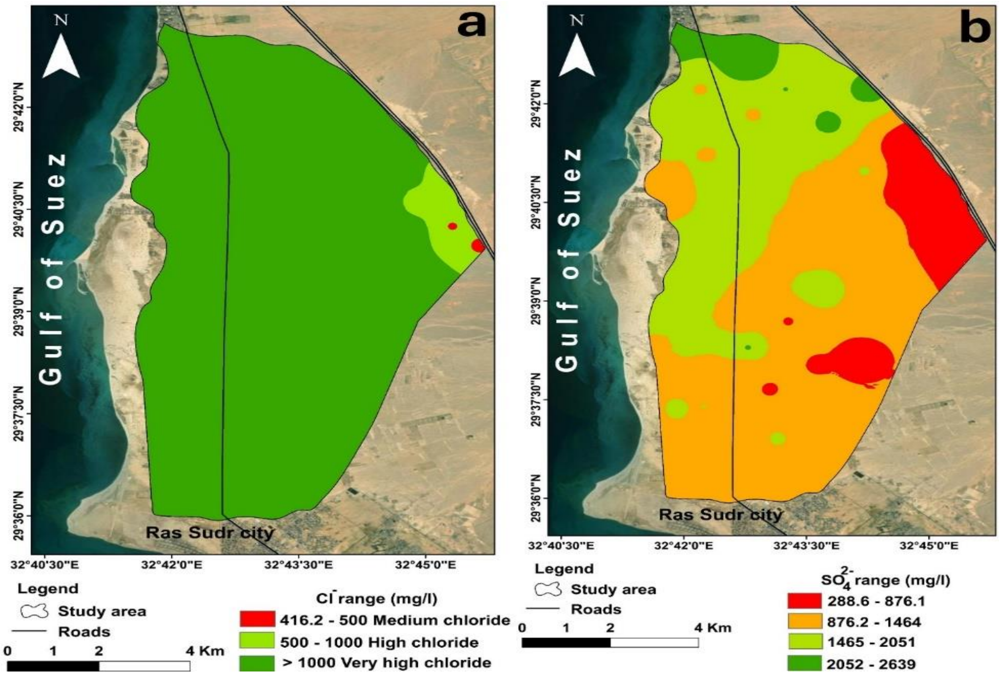

Figure 5: The spatial distribution of: **a**) Cl; **b**) SO_4.

4.1.7. Calcium

Calcium can be obtained from cyclic salt in saltwater, calcareous rock dust, or industrial emissions [61]. Calcium concentrations vary from 105.2 to 915 ppm, with an average concentration of 442.73 ppm. Figure 6a illustrates a pattern of increasing calcium values towards the west and northwest, while values decrease towards the east and at certain sites.

4.1.8. Magnesium

The concentration of magnesium ions ranges from 23 to 572 ppm, with an average of 249.22 ppm. The wells in the northwest areas showed the highest magnesium values, while the lowest magnesium content is typically found in the eastern wells, mainly recharged from the main Wadi channel (Fig. 6b).

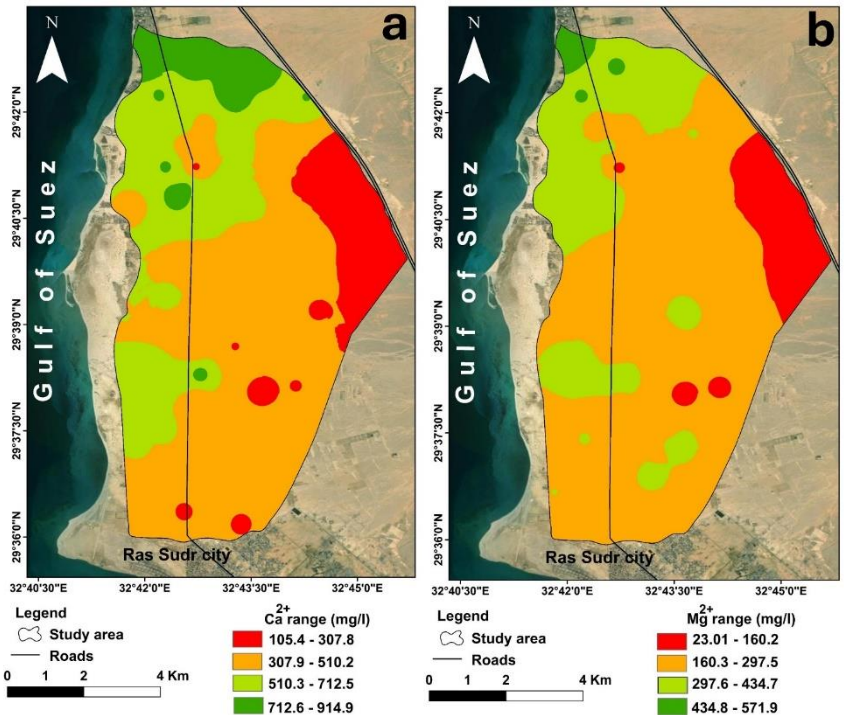

Figure 6: The spatial distribution of: **a**) Ca; **b**) Mg.

4.2. Hydrochemical facies of the Sudr area aquifer

4.2.1. Chadha diagram

Chadha diagram, developed by [62], is a modified version that was plotted to obtain a better understanding of hydrochemistry and distinguish the main water types. The diagram is advantageous for understanding the relationship between essential ions in groundwater [63]. This chart is divided into eight quadrant positions, each of which relates to a distinct hydrochemical facies in groundwater that can be identified by the difference between alkaline earths (Ca^{2+}+Mg^{2+}) and alkali metals (K^++Na^+) is plotted on the X axis, and the difference between weak acidic anions (CO_3^{2-} +HCO_3^-) and strong acidic anions (SO_4^{2-} + Cl^-) is plotted on the Y axis.

Based on the analyzed Chadha diagram (Fig. 7), two main groundwater facies can be distinguished in the investigated area: (1) Na-Cl type, accounting for 98.33% of the total samples, indicates salinization from seawater intrusion (SWI). (2) Ca Mg-Cl type or Ca-Cl type, accounting for 1.67% of the total samples, suggests the reverse ion exchange process that is also considered to be an indication of active seawater intrusion into the aquifer.

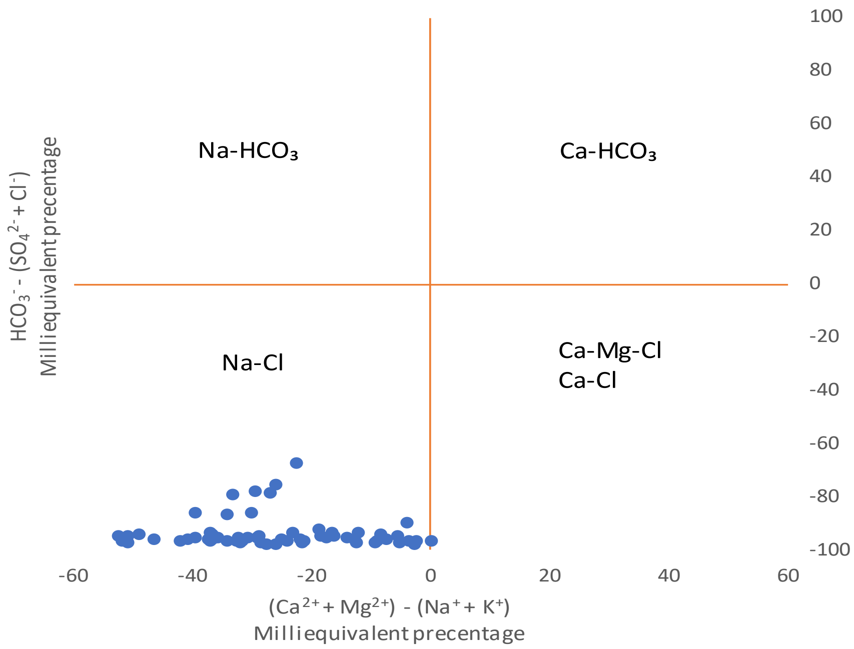

Figure 7: Chadha's diagram showing the main water types in investigated area.

4.2.2. Hydrochemical Facies Evolution Diagram (HFE-D)

The HFE-D is effective for interpreting the intrusion and recovery stages in coastal aquifers to recognize seawater intrusion [64]; [65]. The HFE-D comprises four major types of heteropic facies: Na-Cl, Ca-HCO_3, Ca-Cl_2, and Na-HCO_3. Seawater has a NaCl facies, whereas freshwater has a Ca-HCO_3 facies. The intrusion of seawater leads to the replacement of Na^+ with Ca^{2+}, causing a change in the water composition from Na-Cl to Ca-Cl_2 facies. In contrast, during the freshening phase, the exchange of Ca^{2+} for Na^+ leads to the creation of Na-HCO_3 waters [66].

The Conservative Mixing Line (CML) between fresh water and seawater divides the central box in the diagram into 2 parts: water samples above and to the left of the CML represent the freshening stage, while water samples beneath and to the right of the CML represent the intrusion stage [64,67]. Based on the composition of the sampled waters, various sub-stages related to freshwater and intrusion phases can be recognized. Both freshening sub-stages (f1, f2, f3, f4, and FW), which encompass the freshening process from the beginning to the end, and intrusion sub-stages (i1, i2, i3, i4, and SW), which encompass the intrusion process from the beginning to the end, aid in determining the salinization dynamics of groundwater samples [64,67]. Most of the samples (73.33%) were impacted by SWI, locating beneath the mixing line in the intrusion stage and evolving through the sub-stage sequences (i3 and i4 +SW). The Na-Cl facies are most indicative of the intrusion stage in Figure 8, clearly reflecting the seawater intrusion in groundwater. While the rest of the samples (26.67%) presented above the mixing line in the field of freshening through the dominance of the sub-stage (f1) with Na-Cl facies. As a result, the groundwater samples do not progress to the advanced freshening stage. This can be explained by the recharging of the coastal Sudr aquifer in the main wadi channel toward the east. Additionally, it influences a direct ion-exchange process where sodium ions are released into the groundwater, while calcium ions are absorbed into the aquifer matrix.

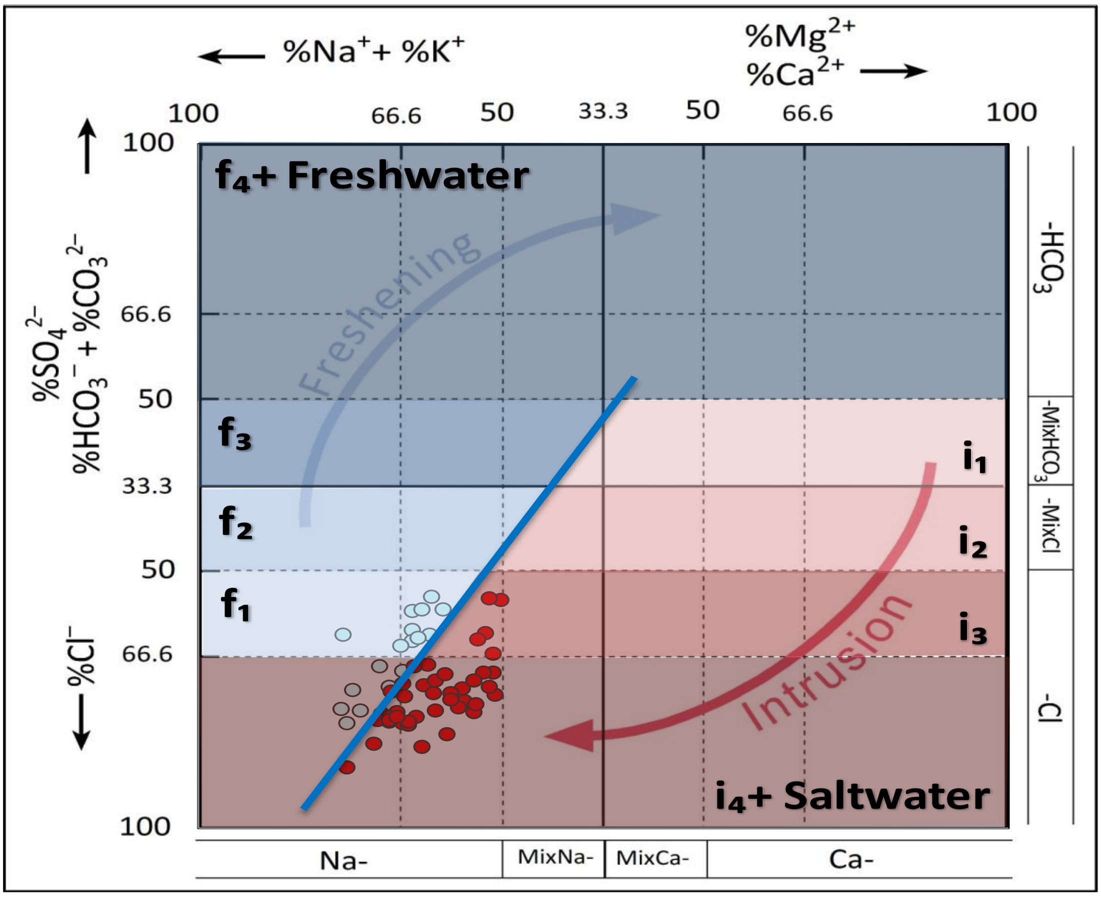

Figure 8: Representation of groundwater samples for Sudr area in HFE-Diagram.

4.2.3. Evaluation of groundwater quality for irrigation uses from 1996 to 2022

The health of plants and the fertility of agricultural soil are greatly affected by the quality of groundwater, which in turn affects irrigation practices [68]. Elevated concentrations of dissolved ions in groundwater can have both physical and chemical effects on plants and soil. This can result in a reduction in osmotic pressure within plant cells, inhibiting water uptake and diminishing irrigation efficiency [69].

4.2.3.1. Sodium adsorption ratio

The Sodium absorption ratio (SAR) is a commonly used indicator to assess the quality of groundwater for irrigation purposes. It is calculated by comparing the concentrations of sodium, calcium, and magnesium ions in the water [45]. In the study area, SAR varies from 4.4 to 21.76 in 1996 and 6.40 to 31.95 in 2022. Most of the groundwater samples in 1996 (71.95%) were found to have no alkalinity hazard and were classified as excellent. However, in 2022, 58.33% of samples were considered as good category as shown in Figure 9 and Table 2, which reflects that seawater intrusion plays a vital role in the rise of the SAR value.

4.2.3.2. Percent sodium

Na% in the study area varies from 35.24 to 66.39 in 1996 and 49.91 to 76.25 in 2022. In 1996, 82.93% of samples were deemed permissible and 13.41% were doubtful, compared to 33.33% considered permissible and 66.67% were doubtful in 2022 (Table 2) (Fig. 10). Elevated levels of sodium in irrigation water can cause clay particles to absorb Na^{+} ions, displacing Mg^{2+} and Ca^{2+} ions. This can decrease soil permeability, leading to inadequate internal drainage that may hinder plant growth [70].

Table 2: Irrigation quality of groundwater based on SAR, Na%, and PI.

Range	Water class	1996	2022
		Percent samples	Percent samples
Sodium adsorption ratio SAR [45]			
<10	Excellent	71.95	10
10-18	Good	23.17	58.33
18-26	Doubtful	4.88	30
>26	Unsuitable	Nil	1.67
Percent sodium Na% [47]			
<20	Excellent	Nil	Nil
20-40	Good	3.66	Nil
40-60	Permissible	82.93	33.33
60-80	Doubtful	13.41	66.67
>80	Unsuitable	Nil	Nil
Permeability index (PI) [50]			
>75	Suitable	18.29	8.33
25-75	Moderate	81.71	91.67
<25	Unsuitable	Nil	Nil

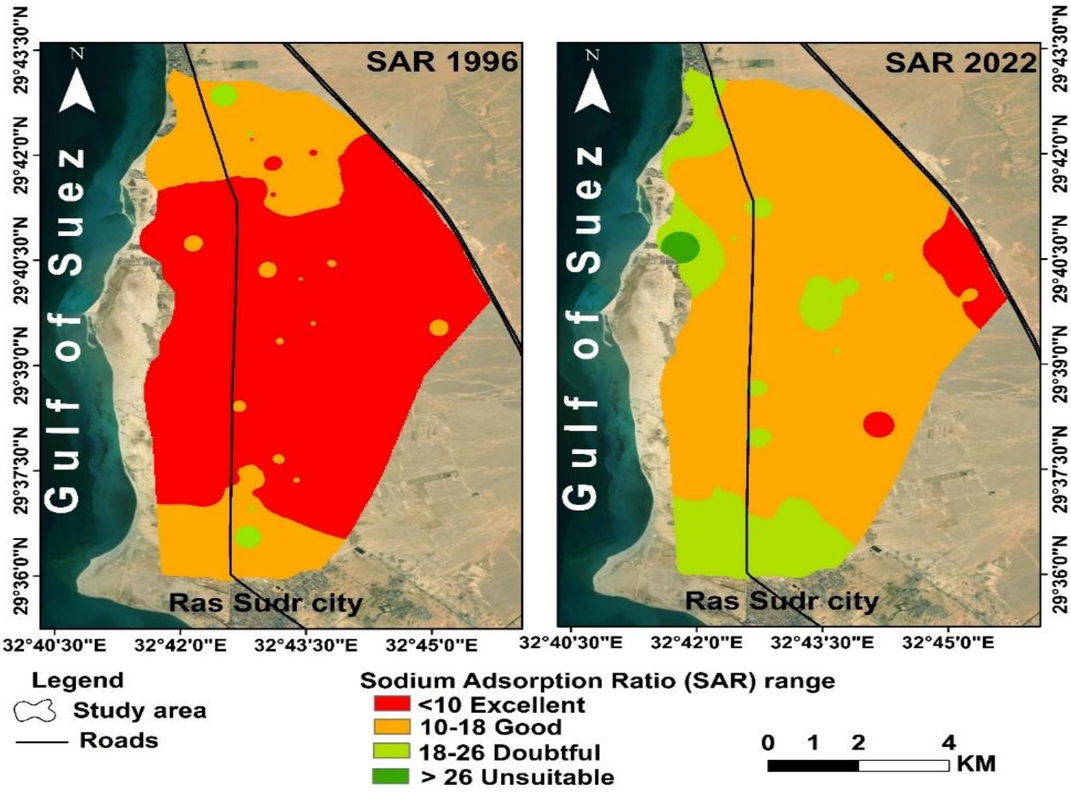

Figure 9: Spatiotemporal variations of SAR (1996–2022).

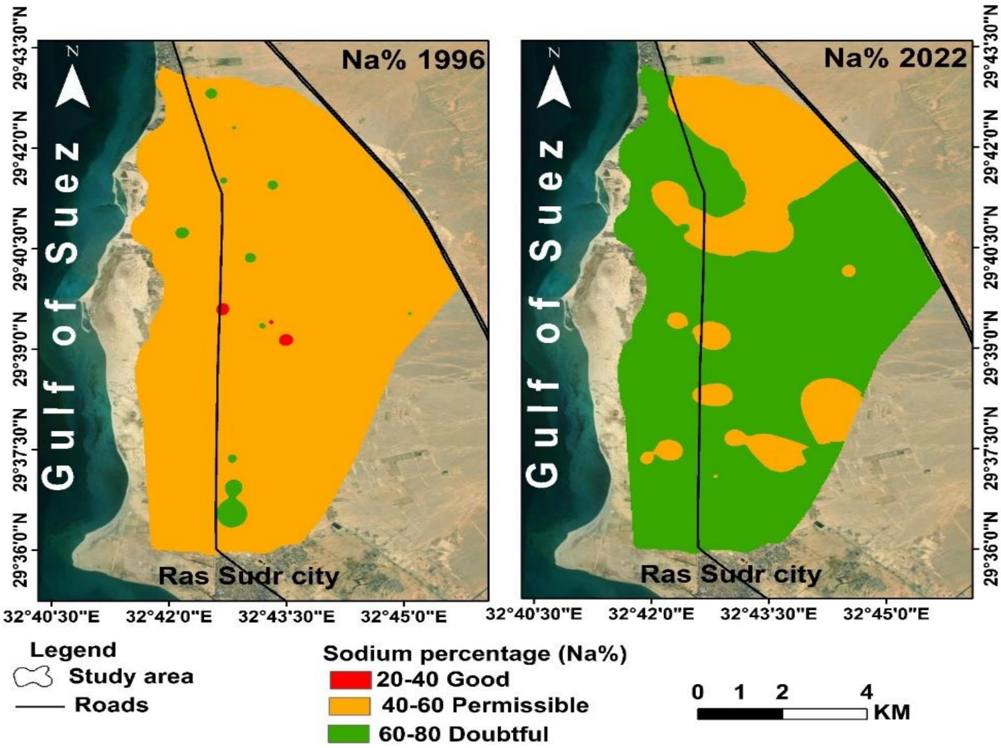

Figure 10: Spatiotemporal variations of Na% (1996–2022).

4.2.3.3. Permeability index

According to [50], waters falling under class >75 and class 25-75 categories are excellent and appropriate for irrigation purposes. On the other hand, class <25 water is unsuitable for irrigation. PI is in range from 55.65 to 87.53 in 1996 and 50.79 to 77.49 in 2022. The study area in 2022 has the highest PI value considered as moderate (25-75), which is 91.67% of samples, while the smallest in 1996, which is 81.71% of samples (Table 2) (Fig. 11). This reflects that the soil's permeability deteriorates over time to more areas.

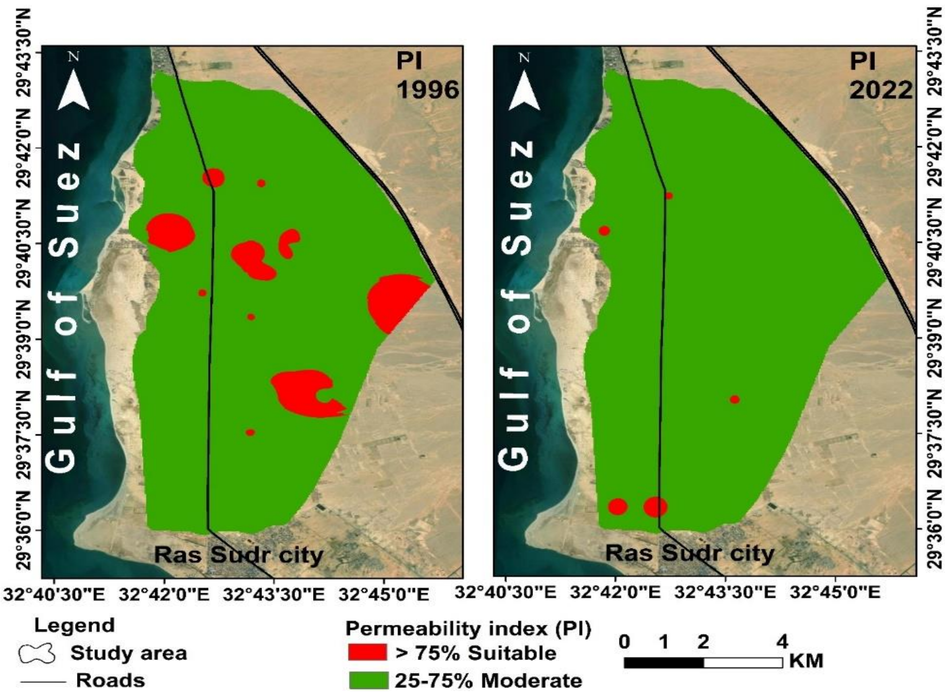

Figure 11: Spatiotemporal variations of PI (1996–2022).

5. Conclusions

The hydrochemical indicators was utilized to evaluate the groundwater quality for irrigation from 1996 to 2022 in the arid coastal aquifer of Sudr area in South Sinai, Egypt. In the study area, groundwater chemistry is characterized by a dominance of Na^+ and Cl^-. The elevated salinity levels in the West and North-West region are predominantly caused by seawater intrusion, erosion of Sabkha and playa, and excessive extraction exceeding the current recharge rate. The East's low salinity values are mainly due to recharge sources from direct percolation of surface runoff water during flash floods that typically occur in the autumn and winter seasons. According to Chadha diagram, 98.33% of the total samples showed Na-Cl type indicating salinization from seawater intrusion. Furthermore, SWI impacted 73.33% of the samples by HFE-Diagram. The findings of spatiotemporal variation over 26 years showed that in 1996, 71.95% of samples in the SAR were classified as excellent, whereas in 2022, 58.33% were categorized as good. Na% in 1996, 82.93% of samples were classified as permissible, while 13.41% were in doubtful class. In contrast, only 33.33% were deemed permissible in 2022, with the majority of samples, 66.67%, being classified as doubtful. In 2022, PI exhibited the highest value within the moderate range, representing 91.67% of samples. Conversely, in 1996, the smallest PI value was recorded, comprising 81.71% of samples. For maintaining sustainable groundwater quality, regular monitoring of seawater intrusion is essential in coastal aquifers.

6. Conflicts of interest

There are no conflicts to declare.

7. Data availability statement

The data will be provided on request.

8. Acknowledgements

Ahmed Sedik has been generously supported by the American people through the United International for Agency States Development (USAID-Grant No. 72026319CA00001). The contents are the responsibility of the authors and do not necessarily reflect the views of USAID or the United States Government. The authors would like to thank the Environmental Geophysics Lab (ZEGL), Geology Department, Faculty of Science, Zagazig University, Egypt, and Water-Quality Lab in Desert Research Center, Cairo, Egypt for their cooperation and supporting this work.

References

[1] L. Tulipano, D.M. Fidelibus & A. Panagopoulos. (2005) Groundwater Management of Coastal Karstic Aquifers.

[2] E. Custodio. (2010). Costal Aquifers of Europe: An Overview. Hydrogeol J., 18, 269–280, doi:10.1007/s10040-009-0496-1.

[3] A.D. Werner, M. Bakker, V.E.A. Post, A. Vandenbohede, C. Lu, B. Ataie-Ashtiani, C.T. Simmons & D.A. Barry. (2013). Seawater Intrusion Processes, Investigation and Management: Recent Advances and Future Challenges. Adv Water Resour, 51, 3–26, doi:10.1016/j.advwatres.2012.03.004.

[4] P.H. Gleick, G.H. Wolff, H. Cooley, M. Palaniappan, A. Samulon, E. Lee, J. Morrison & D. Katz. (2013). The World's Water 2006-2007: The Biennial Report on Freshwater Resources; Island Press, ISBN 1597269514.

[5] M. Mastrocicco & N. Colombani. (2021). The Issue of Groundwater Salinization in Coastal Areas of the Mediterranean Region: A Review. Water (Switzerland), 13, doi:10.3390/w13010090.

[6] K. Walraevens, A. Chaouni Alia, N. EL Halimi, E. Beeuwsaert & W. De Breuck. (1997). Investigation de La Salinisation de La Plaine de Bou-Areg (Maroc Nord-Oriental). In Proceedings of the Rabat Symposium S4; International Association of Hydrological Sciences (IAHS); Vol. 243, pp. 211–220.

[7] E. Custodio. (2002). Aquifer Overexploitation: What Does It Mean? Hydrogeol J, 10, 254–277, doi:10.1007/s10040-002-0188-6.

[8] S. Faye, P. Maloszewski, W. Stichler, P. Trimborn, S.C. Faye & C.B. Gaye. (2005). Groundwater Salinization in the Saloum (Senegal) Delta Aquifer: Minor Elements and Isotopic Indicators. Science of the Total Environment, 343, 243–259, doi:10.1016/j.scitotenv.2004.10.001.

[9] S. Khayat, H. Hötzl, S. Geyer & W. Ali. (2006). Hydrochemical Investigation of Water from the Pleistocene Wells and Springs, Jericho Area, Palestine. Hydrogeol J, 14, 192–202, doi:10.1007/s10040-004-0399-0.

[10] G. Steyl & I. Dennis. (2010). Review of Coastal-Area Aquifers in Africa | Recensement Des Aquifères Côtiers En Afrique. Hydrogeol J, 18, 217–225, doi:10.1007/s10040-009-0545-9.

[11] T. Agardy, J. Alder, P. Dayton, S. Curran, A. Kitchingman, M. Wilson, A. Catenazzi, J. Restrepo, C. Birkeland & S. Blaber. (2005). Coastal Systems. Ecosystems and human well-being: current state and trends, 1, 513–549.

[12] F. Ferrario, M.W. Beck, C.D. Storlazzi, F. Micheli, C.C. Shepard & L. Airoldi. (2014). The Effectiveness of Coral Reefs for Coastal Hazard Risk Reduction and Adaptation. Nat Commun, 5, doi:10.1038/ncomms4794.

[13] N.A. Abo Shaala. (2016). Hydrologic Assessment of Wadi Sudr and Vicinities, South Sinai, Egypt. (Doctoral dissertation, Ph. D. Thesis, Faculty of Science, Ain Shams University, Cairo, Egypt).

[14] A.C. Mills & A. Shata. (1989). Ground-Water Assessment of Sinai, Egypt. Groundwater, 27, 793–801, doi:10.1111/j.1745-6584.1989.tb01043.x.

[15] B. Askri, A.T. Ahmed, R.A. Al-Shanfari, R. Bouhlila & K.B.K. Al-Farisi. (2016). Isotopic and Geochemical Identifications of Groundwater Salinisation Processes in Salalah Coastal Plain, Sultanate of Oman. Chemie der Erde, 76, 243–255, doi:10.1016/j.chemer.2015.12.002.

[16] H. Bouzourra, R. Bouhlila, L. Elango, F. Slama & N. Ouslati. (2015). Characterization of Mechanisms and Processes of Groundwater Salinization in Irrigated Coastal Area Using Statistics, GIS, and Hydrogeochemical Investigations. Environmental Science and Pollution Research, 22, 2643–2660, doi:10.1007/s11356-014-3428-0.

[17] R.A. Awwad, T.N. Olsthoorn, Y. Zhou, S. Uhlenbrook & E. Smidt. (2008). Optimum Pumping-Injection System for Saline Groundwater Desalination in Sharm El Sheikh; Water Mill Working Paper.

[18] A.A. El-Fiky. (2010). Hydrogeochemical Characteristics and Evolution of Groundwater at the Ras Sudr-Abu Zenima Area, Southwest Sinai, Egypt. Journal of King Abdulaziz University, Earth Sciences, 21, 79–109, doi:10.4197/Ear.21-1.4.

[19] H. Isawi, M.H. El-Sayed, M. Eissa, O. Shouakar-Stash, H. Shawky & M.S. Abdel Mottaleb. (2016). Integrated Geochemistry, Isotopes, and Geostatistical Techniques to Investigate Groundwater Sources and Salinization Origin in the Sharm EL-Shiekh Area, South Sinia, Egypt. Water Air Soil Pollut, 227, doi:10.1007/s11270-016-2848-5.

[20] M.A. Eissa, H.H. Mahmoud, O. Shouakar-Stash, A. El-Shiekh & B. Parker. (2016). Geophysical and Geochemical Studies to Delineate Seawater Intrusion in Bagoush Area, Northwestern Coast, Egypt. Journal of African Earth Sciences, 121, 365–381, doi:10.1016/j.jafrearsci.2016.05.031.

[21] S. Selvam, G. Manimaran & P. Sivasubramanian. (2013). Hydrochemical Characteristics and GIS-Based Assessment of Groundwater Quality in the Coastal Aquifers of Tuticorin Corporation, Tamilnadu, India. Appl Water Sci, 3, 145–159, doi:10.1007/s13201-012-0068-8.

[22] S. Barua, B.P. Mukhopadhyay & A. Bera. (2021). Hydrochemical Assessment of Groundwater for Irrigation Suitability in the Alluvial Aquifers of Dakshin Dinajpur District, West Bengal, India. Environ Earth Sci, 80, 514.

[23] A.F. Khan, K. Srinivasamoorthy & C. Rabina. (2020). Hydrochemical Characteristics and Quality Assessment of Groundwater along the Coastal Tracts of Tamil Nadu and Puducherry, India. Appl Water Sci, 10, 1–21.

[24] S.K. Srivastava. (2019). Assessment of Groundwater Quality for the Suitability of Irrigation and Its Impacts on Crop Yields in the Guna District, India. Agric Water Manag, 216, 224–241.

[25] N. Aziane, A. Khaddari, M. IbenTouhami, A. Zouahri, H. Nassali & M.S. Elyoubi. (2020). Evaluation of Groundwater Suitability for Irrigation in the Coastal Aquifer of Mnasra (Gharb, Morocco). Mediterranean Journal of Chemistry, 10, 197–212.

[26] M.E. Gabr, H. Soussa & E. Fattouh. (2021). Groundwater Quality Evaluation for Drinking and Irrigation Uses in Dayrout City Upper Egypt. Ain Shams Engineering Journal, 12, 327–340.

[27] M.M. Zafar, M.A. Sulaiman, R. Prabhakar & A. Kumari. (2022). Evaluation of the Suitability of Groundwater for Irrigational Purposes Using Irrigation Water Quality Indices and Geographical Information Systems (GIS) at Patna (Bihar), India. International Journal of Energy and Water Resources, doi:10.1007/s42108-022-00193-1.

[28] M.M. Said. (2004). Geochemistry of Groundwater in Coastal Areas, South Sinai, Egypt.

[29] T.A. Abdel-Latief & A.M.M. Al-Temamy. (2008). Study of the Impact of Groundwater Discharge on the Brackish-Saline Interface Using Two–Dimensional Resistivity Imaging in the Delta of Wadi Sudr, Western Sinai, Egypt. Journal Desert Research, 58, 1–17.

[30] C. Conoco. (1987). Geological Map of Egypt, Scale 1: 500,000-NF 36 NE-Bernice, Egypt. The Egyptian General Petroleum Corporation, Cairo.

[31] N.A. Morad. (2000). Rainfall-Runoff Relationship in Mountainous Areas; Case Study Wadi Sudr (Doctoral Dissertation, M. Sc. Thesis, Faculty of Engineering, Ain Shams University, Cairo, Egypt).

[32] E. El Sayed, Y. L. Ismail & M. A. Gomaa. (1999). Hydrogeological Investigation in the Coastal Area of the Delta of Wadi Sudr, Gulf of Suez, South Sinai, Egypt. Bull. Fac. of Science. Assuit Univ, 143-160.

[33] A.A. Abdel-Hafez. (2001). Chemical Evaluation and Possible Treatment of Sea Water Intrusion in the Groundwater in Some Coastal Areas. South Sinai (Doctoral Dissertation, M. Sc. Thesis Fac of Science, Al Azhar Univ (Girls). 223pp.

[34] H.K. Garamoon. (1987). Hydrological Studies of Sudr Area, Southern Sinai, Egypt (Doctoral Dissertation, M. Sc. Thesis, Faculty of Science, Science, Ain Shams University, Egypt).

[35] S.M.M. Ibrahim. (2012). Monitoring of Seawater Encroachement in the Delta of Wadi Sudr, South Sinai, Egypt. Assiut University Journal of Geology, 41, 23–60.

[36] M.A. El-Bihery. (2009). Groundwater Flow Modeling of Quaternary Aquifer Ras Sudr, Egypt. Environmental Geology, 58, 1095–1105, doi:10.1007/s00254-008-1589-1.

[37] F.H. Rainwater & L.L. Thatcher. (1960). Methods for Collection and Analysis of Water Samples; US Government Printing Office.

[38] J.D. Rhoades. (1972). Quality of Irrigation Water. Soil Sci, 113:277-284.

[39] M.J. Fishman & L.C. Friedman. (1985). Methods for Determination of Inorganic Substances in Water and Fluvial Sediments, US Geological Survei Book 5, Chapter A1. Open File Report 84: 85–495 Denver Colorado USA for Hydrogen Isotope Analysis. Anal Chem, 63, 910–912.

[40] J.D. Hem. (1991). Study and Interpretation of the Chemical Characteristics of Natural Water. Book 2254, 3rd Edition, Scientific Pub, Jodhpur, India.

[41] APHA (American Public Health Association). (1998). Standard Methods for the Examination of Water and Wastewater, Twentieth Ed., p. 46p Washington, DC.

[42] ASTM (American Society for Testing and Materials). (2002). Water and Environmental Technology. Annual Book of ASTM Standards. U.S.A. Sec., 11: 11.01 and 11.02, West Conshohocken.

[43] P.A. Domenico & F.W. Schwartz. (1990). Physical and Chemical Hydrogeology. Wiley, New York, p. 824.

[44] D.K. Todd & L.W. Mays. (2004). Groundwater Hydrology; John Wiley & Sons; ISBN 0471059374.

[45] R.S. Ayers & D.W. Westcot. (1985). Water Quality for Agriculture; Food and Agriculture Organization of the United Nations Rome; Vol. 29; ISBN 9251022631.

[46] L.A. Richards. (1954). Diagnosis and Improvement of Saline and Alkali Soils; US Government Printing Office.

[47] Lv. Wilcox. (1955). Classification and Use of Irrigation Waters; US Department of Agriculture.

[48] W.P. Kelley. (1951). Alkali, Soils, Their Formation. Properties and Reclamation, 141–143.

[49] K.S. Rawat, S.K. Singh & S.K. Gautam. (2018). Assessment of Groundwater Quality for Irrigation Use: A Peninsular Case Study. Appl Water Sci, 8, 1–24.

[50] L.D. Doneen. (1964). Notes on Water Quality in Agriculture; Department of Water Science and Engineering, University of California, Davis.

[51] T. Shirabe. (2012). Prescriptive Modeling with Map Algebra for Multi-Zone Allocation with Size Constraints. Comput Environ Urban Syst, 36, 456–469, doi:https://doi.org/10.1016/j.compenvurbsys.2011.12.003.

[52] N.U. Kura, M.F. Ramli, S. Ibrahim, W.N.A. Sulaiman & A.Z. Aris. (2014). An Integrated Assessment of Seawater Intrusion in a Small Tropical Island Using Geophysical, Geochemical, and Geostatistical Techniques. Environmental Science and Pollution Research, 21, 7047–7064, doi:10.1007/s11356-014-2598-0.

[53] T. Subramani, L. Elango & S.R. Damodarasamy. (2005). Groundwater Quality and Its Suitability for Drinking and Agricultural Use in Chithar River Basin, Tamil Nadu, India. Environmental Geology, 47, 1099–1110.

[54] WHO. (2017). Guidelines for Drinking-Water Quality: Fourth Edition Incorporating the First Addendum. World Health Organization, Geneva.

[55] S.N. Davis, R.J.M. De Wiest. (1966). Hydrogeology.

[56] R.A. Freeze & J.A. Cherry. (1979). Groundwater; 0-13-365312-9; Prentice-Hall, ISBN 9780133653120.

[57] A. Phocaides. (2000). Technical Handbook on Pressurized Irrigation Techniques. FAO, Rome, 372.

[58] BK. Handa (1969). Description and Classification of Media for Hydrogeochemical Investigations. In: Symposium on Ground Water Studies in Arid and Semiarid Regions, Roorkee.

[59] C. Sawyer & P. McCarthy. (1967). Chemical and Sanitary Engineering

[60] G.G. Taylor & M.M. Oza. (1954). Geological Survey of India. Bull Series B, 45, 29.

[61] I.F. EL Fayoumy. (1968). Geology of Groundwater Supplies in the Region East of the Nile Delta Ph.D. Thesis, Fac. Sci. Cairo Univ. 201p.

[62] D.K. Chadha. (1999). A Proposed New Diagram for Geochemical Classification of Natural Waters and Interpretation of Chemical Data. Hydrogeol J, 7, 431–439, doi:10.1007/s100400050216.

[63] U.D. Ijioma. (2021). Delineating the Impact of Urbanization on the Hydrochemistry and Quality of Groundwater Wells in Aba, Nigeria. J Contam Hydrol, 240, 103792, doi:10.1016/J.JCONHYD.2021.103792.

[64] E. Giménez-Forcada. (2019). Use of the Hydrochemical Facies Diagram (HFE-D) for the Evaluation of Salinization by Seawater Intrusion in the Coastal Oropesa Plain: Comparative Analysis with the Coastal Vinaroz Plain, Spain. HydroResearch, 2, 76–84, doi:https://doi.org/10.1016/j.hydres.2019.11.007.

[65] A. Parisi, M.R. Alfio, G. Balacco, C. Güler & M.D. Fidelibus. (2023). Analyzing Spatial and Temporal Evolution of Groundwater Salinization through Multivariate Statistical Analysis and Hydrogeochemical Facies Evolution-Diagram. Science of The Total Environment, 862, 160697, doi:https://doi.org/10.1016/j.scitotenv.2022.160697.

[66] R. Chandrajith, U.G.C. Bandara, S. Diyabalanage, S. Senaratne & J.A.C. Barth. (2022). Application of Water Quality Index as a Vulnerability Indicator to

Determine Seawater Intrusion in Unconsolidated Sedimentary Aquifers in a Tropical Coastal Region of Sri Lanka. Groundw Sustain Dev, 19, 100831, doi:https://doi.org/10.1016/j.gsd.2022.100831.

[67] E. Giménez-Forcada. (2014). Space/Time Development of Seawater Intrusion: A Study Case in Vinaroz Coastal Plain (Eastern Spain) Using HFE-Diagram, and Spatial Distribution of Hydrochemical Facies. J Hydrol (Amst), 517, 617–627, doi:https://doi.org/10.1016/j.jhydrol.2014.05.056.

[68] S. Gugulothu, N. Subbarao, R. Das & R. Dhakate. (2022). Geochemical Evaluation of Groundwater and Suitability of Groundwater Quality for Irrigation Purpose in an Agricultural Region of South India. Appl Water Sci, 12, doi:10.1007/s13201-022-01583-w.

[69] A. Sarkar, B. Paul & G.K. Darbha. (2022). The Groundwater Arsenic Contamination in the Bengal Basin-A Review in Brief. Chemosphere, 299, doi:10.1016/j.chemosphere.2022.134369.

[70] P. Ravikumar, R.K. Somashekar & M. Angami. (2011). Hydrochemistry and Evaluation of Groundwater Suitability for Irrigation and Drinking Purposes in the Markandeya River Basin, Belgaum District, Karnataka State, India. Environ Monit Assess, 173, 459–487.